The Use of Regolith Simulant as a Material for Building Functional Sensors in Extreme Environments

Sofia I. de Hoffmann*, Lexi J. Greenwood†, and Seetha Raghavan‡
Embry-Riddle Aeronautical University, Daytona Beach, Florida, USA

Space exploration is evolving and demands the development of advanced materials capable of performing in such an environment. This paper explores the potential of using lunar regolith simulants for the development of functional sensors to be used in extreme environments. Lunar Highland Simulant (LHS) was used to 3D print samples via digital light processing (DLP). The challenge of in-space manufacturing of functional sensors is to find a reliable and efficient method to transform regolith into materials that can perform its function in space conditions. This study demonstrates that a photosensitive resin incorporated with a 10 wt% regolith simulant produces characteristic Raman peaks representing different minerals within the simulant. An in-situ Raman study with an LHS sample under compression demonstrated shifts in the Raman peaks with applied stress. The shift of these peaks can be utilized as a sensing property when calibrated with stress. The results provide an insight into the use of in-situ resources for in-space manufacturing of functional sensors.

I. Nomenclature

$LMS-1D$	=	Lunar Mare Dust Simulant
$LHS-1D$	=	Lunar Highland Dust Simulant
DLP	=	Digital Light Processing

II. Introduction

The surface of the moon consists of lunar regolith which is a very fine and jagged material. This loose and fragmented material has many possible future in-situ applications, from construction [1] to its potential as a source of rocket propellant [2]. The growing interest in lunar exploration and beyond creates a need for such technologies that utilize planetary regolith for efficiency and economic purposes [3, 4] . In this work, we explore the opportunities presented by in-situ utilization of regolith for the creation of functional sensors using Raman spectroscopy.

Raman spectroscopy works by using a laser to excite molecules within the given sample. Using laser light, a small portion gets inelastically scattered into different wavelengths to create the Raman scatter. A Raman spectrum is the result which can show a variety of peaks, depending on the material. Each peak represents a different molecular bond vibration that can vary in wavelength and intensity. This non-destructive testing method gives a better look at the composition of nanomaterials as well as information regarding its structure and bonding [5, 6]. These resultant peaks can also be used to observe certain environmental effects by investigating changes in their peak properties.

Because access to real regolith from the Apollo missions is limited, a simulant is commonly used in its place for testing. For this study, a Lunar Highland Simulant (LHS) was used. Its mineralogy in weight percentages and its known corresponding Raman peaks is summarized within Table 1. Here, its sensing capabilities are under investigation, specifically those in regards to compression. By using Raman spectroscopy, spectral emissions can be observed before and during the loading of regolith samples via compression testing [7]. Through this experimentation, it is possible to observe any shifts in peaks, changes in intensity or changes in line width that may occur. This will provide information on the effectiveness of this methodology to create sensing capabilities using lunar regolith.

*Undergraduate Student, Aerospace Engineering Embry-Riddle Aeronautical University, AIAA student member
†Undergraduate Student, Aerospace Engineering, Embry-Riddle Aeronautical University, AIAA student member
‡Professor and Associate Dean, Aerospace Engineering, Embry-Riddle Aeronautical University, AIAA Associate Fellow, seetha.raghavan@erau.edu.

Table 1 Mineral composition of LHS regolith simulant used within this study as well as the known Raman peaks of the minerals within this lunar simulant (adapted from [8])

Mineral	LHS wt%	Known Raman Peaks (cm^{-1})
Pyroxene	0.3	
(Ortho)		331,388,657,673,1001 [9]
		338,679,1007 [10]
		225-325,375-490,650-750,800-1100 [11].
		660,678,1006 [12]
(Clino)		317,663,995 [10]
		306,339,372,653,995 [9]
		230,327,255,360,393,665,1010 [11]
		665,1005 [12]
Glass-rich Basalt	24.7	757,970 [10]
Anorthosite	74.4	485-488,505,557-564[13]
		504 [9]
		483,503 [12]
Olivine	0.2	815,847 [9]
		819,848 [10]
		810,850,914,950 [11]
		242,295,372,558,817,840,921 (Fayalite) [14]
		230,307,440,588,620,826,858,883,967(Forsterite) [14]
		826,856 [12]
Ilmenite	0.4	681 [10]
		600-700 [12]

III. Manufacturing and Experimental Methods

The manufacturing section summarizes the processing of the samples and is described in more detail in our previous work [8, 15]. The experimental methods describe the set up used to evaluate the manufactured samples by assessing the particle behavior under compression loads. The setup consists of an integration between a compression test and Raman spectroscopy scanning system as shown in Fig 1.

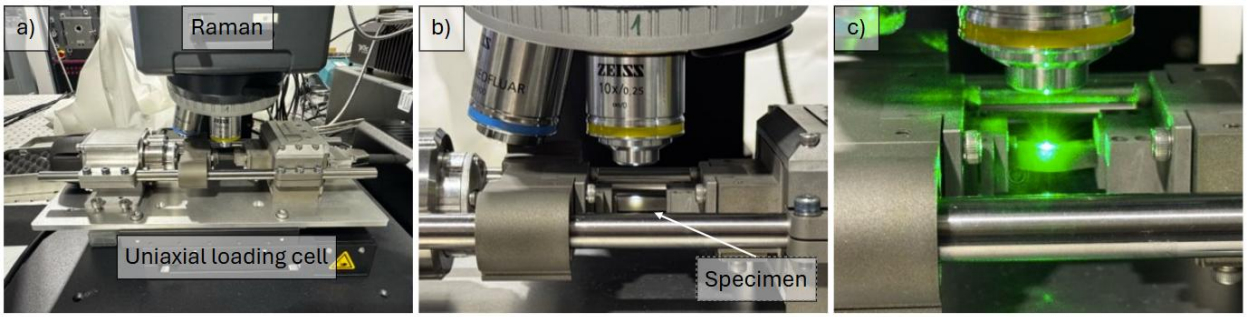

Fig. 1 a) Experimental setup with Raman and light microscope function, equipped with uniaxial loading cell; b) High magnification of experimental setup with mounted specimen in uniaxial loading cell; c) Loaded specimen exposed to a 532 nm laser

A. Sample Manufacturing

Regolith simulant composites (LHS-1D) were manufactured by 3D printing with DLP. 10 wt% regolith was chosen for manufacturing to ensure sufficient concentration to provide Raman intensity without issues of agglomeration [16]. The epoxy resin and LHS were mixed together for three minutes, using the THINKY mixer AR-100. The mixture was then 3D printed using a DLP printer with a 5 μm layer thickness and cured with 405 nm UV light for 6 seconds per layer. For postprocessing, the samples were washed with isopropyl alcohol and additional UV curing for three minutes. The sample can be observed in Fig 1b. The dimensions of the sample was 16 mm X 3.8 mm X 3.8 mm.

B. Raman Spectroscopy

The Raman measurements were obtained using a WITec Alpha 300R Confocal Raman microscope. A laser with an excitation wavelength of 532 nm, and a 10x magnification objective were used to obtain the scans which are collected with a 1800 g/mm grating onto a CCD. An image of the Raman setup with the laser in operation is shown in Fig 1c. The data was obtained by tracking a Plagioclase particle in the LHS-1D sample, identified by characteristic peaks and by doing a single spectrum at said particle with 20 accumulations. The data from the Raman scans present themselves a series of peaks that can be identified from Table 1. These peaks are then investigated for variations in peak position when the sample is loaded in compression.

C. Compression Testing

To evaluate the sensor functionality to compressive loads the DLP LHS-1D 10 wt% was placed in the Psylotech load frame, as shown in Fig 1a. An estimation of the maximum compression load was determined to be approximately 80 MPa using the modulus of the cured resin as a baseline. The sample was therefore tested up to 52 MPa. The first 30 MPa were loaded in steps of 1 MPa and after that the intervals increased to 3 MPa until the 52 MPa was reached. For each increment, Raman scans of the sample were taken. Fig 2 shows the load profile, as well as images of the sample before and after experiencing the compression force. It was observed that the sample started buckling as the applied stress approached 52 MPa.

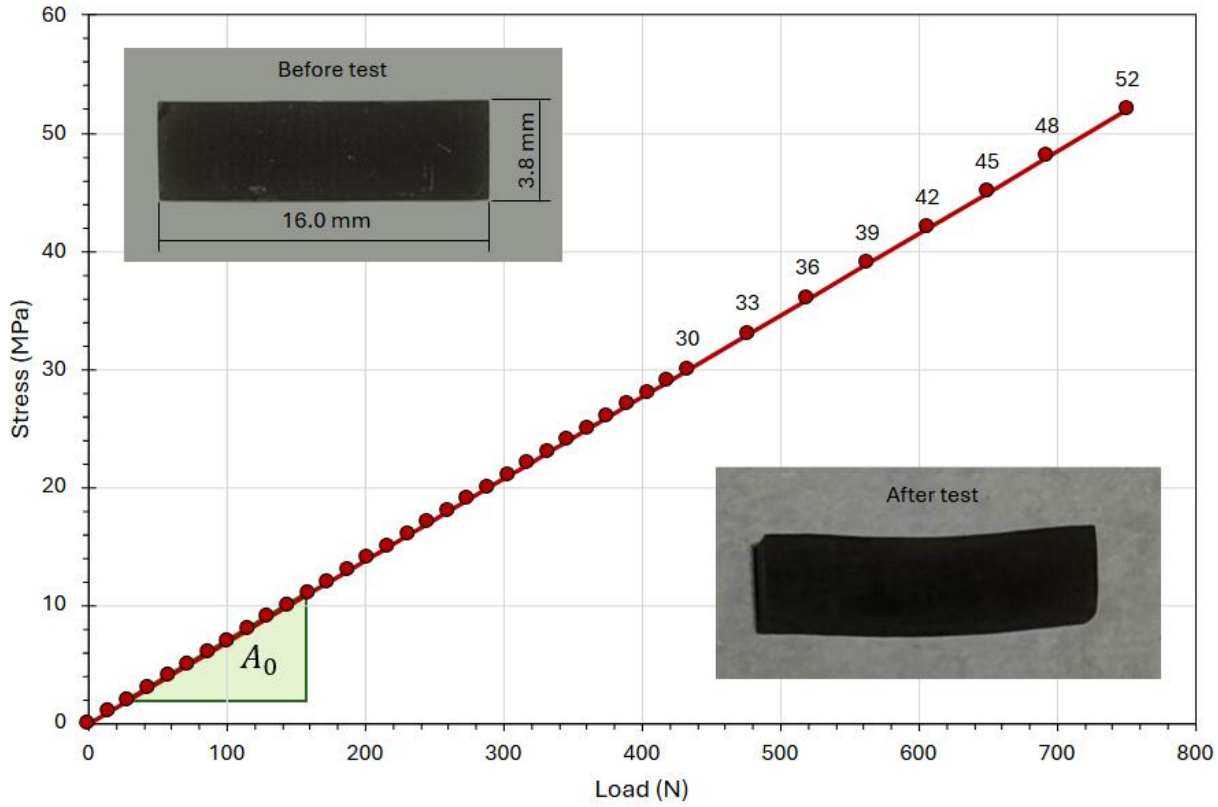

Fig. 2 Experimental matrix for loading rectangular specimens of LHS-DLP specimens in an uniaxial loading cell, stress in MPa vs. the load in Newton. The slope corresponds with the loaded cross-sectional area A_0 (14.44 mm²)

IV. Results and Discussion

The results obtained from the Raman spectrometer and the compression tests in the in-situ measurement configuration are presented and discussed in this section.

A. Raman Spectroscopy

Raman spectroscopy was used to obtain the molecular structural behavior and stress-induced variations in the DLP LHS sample. The spectra collected at different compression stresses (0 MPa to 52 MPa) show a shift in the characteristic Raman peaks identified to be that of Plagioclase as shown in Fig 3a. The focus was set at the second more intense peak of the Plagioclase doublet which we identify as the 507 cm^{-1} peak and the graph was zoomed in into the selected range as shown in Fig 3b. This peak provides an initial measurement of 507.5 cm^{-1} at 0 MPa and then produced a rightward shift with increasing applied stress until it reached 510.4 cm^{-1} at 39 MPa. As Raman spectroscopy provides insight into the atomic structure of particles, there are two factors that influence the peaks:

(i) The mechanical parameters, such as atomic mass, bond strength, or geometry (interatomic distance)

(ii) The charge transfer parameter, such as band structure, or electronic insertion [17]

The compression force does not has any effect on the charge of the particle but it does affect the geometry by making the interatomic distances smaller. This explains the existence of the rightward shift. At 52 MPa, the same peak can be observed at 508.0 cm-1 and buckling can be observed in the image from Fig 2. The buckling of the sample modifies the way the stress is acting on it. This allows for the interatomic distance of the particle to increase, which generates the leftward shift. The buckling and the left shift of the Raman peak at 52 MPa would indicate the failure point of the sample.

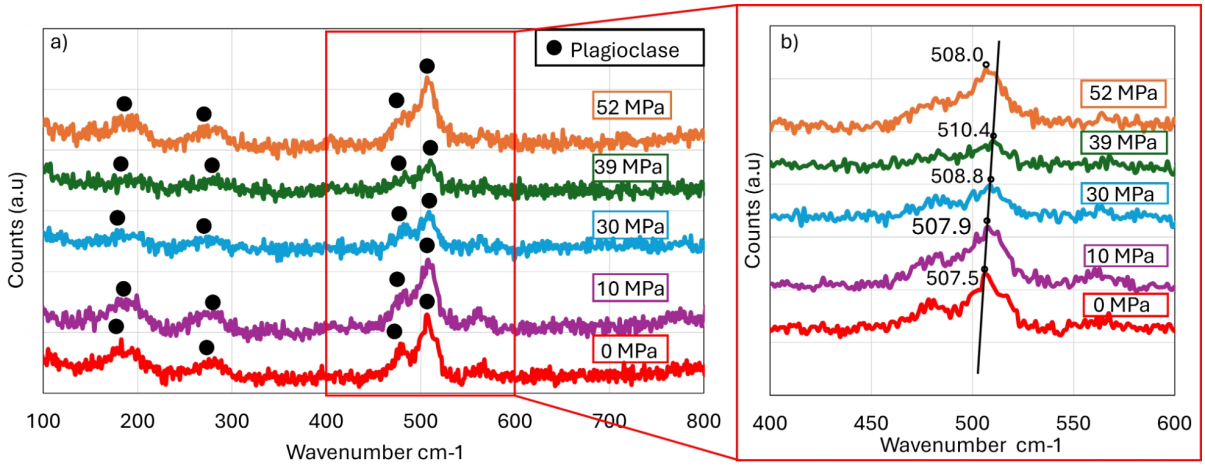

Fig. 3 a) Plagioclase Raman peaks obtained from 5 different loading ; b) Zoomed in peak to analyze tendency

B. Compression Testing

As previously stated, there is a correlation between the right shifting of the Raman peaks and the stress the sample is undergoing. This relationship is described in Fig 4 which shows the obtained slope for the peak shifts at different loads. The slope represents the sensitivity of the sample to mechanical loading, providing insight on its use as a stress-sensing material [18]. This slope also known as the piezospectroscopic (PS) coefficient [19] is determined to be 55.7 cm^{-1}/GPa for the 507 cm^{-1} Plagioclase peak. The graph shows a positive linear trend, this confirms that within this range the DLP sample exhibits elastic behavior. The steeper the slope the more sensitive the material is, while the shallower the less responsive to applied stress. For this sample a moderate slope can be observed, not to steep and not to shallow, which indicates that the material can detect moderate stress changes with measurable Raman peaks. Although, the effectiveness decreases at higher loads.

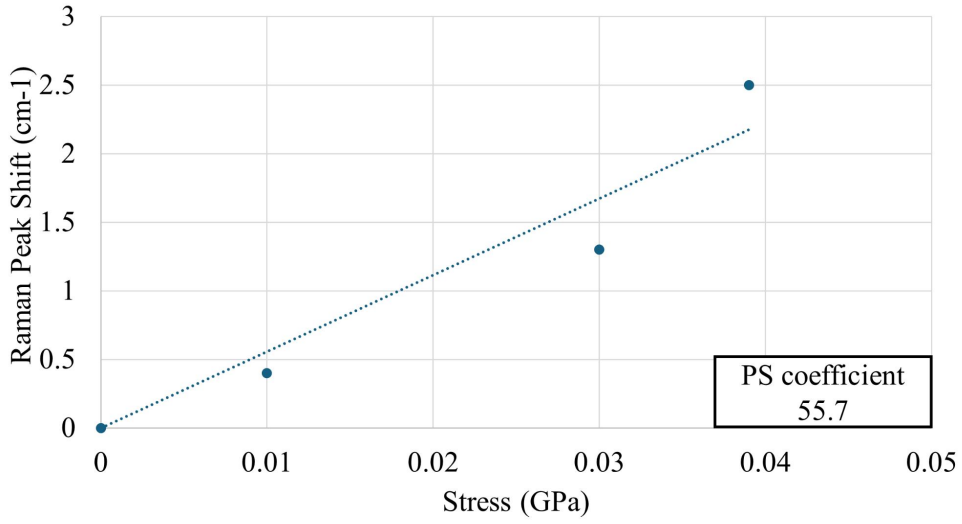

Fig. 4 Slope between the Raman shift and the stress provides the piezospectroscopic coefficient of the 507cm^{-1} Plagioclase peak

The fact that the particle being measured with Raman is experiencing a shift when load is applied indicates there is good bonding between the particles of LHS in the resin, since this means the particle is also experiencing the compression in addition to the resin through load transfer. The shift for 52 MPa was not considered in this plot because

the sample was no longer in uniaxial compression at this applied stress and this data point is a deviation from elastic behavior. This deviation is likely due to the mechanical failure (buckling) the sample experienced at that load.

V. Conclusion

This study demonstrated the potential of using LHS-1D to manufacture functional sensors in extreme environments. The DLP manufacturing process was used to create samples with 10 wt% LHS and epoxy. The Raman spectroscopy of this sample provided measurable shifts in the characteristic spectra of Plagioclase under applied compressive stress. The observed rightward shift of those peaks reveals a stress-dependent response with a PS coefficient of $55.7 cm^{-1}/GPa$. This indicates the possibility of using regolith-based composites as sensing materials. However, there was a leftward shift at 52 MPa, and a buckling of the sample, suggesting a limit to the allowable stress. These findings provide insight into the use of in-situ materials for space sensor applications. Further work will explore optimizing the material composition and processing techniques to understand the mechanical behavior.

Acknowledgments

This material is based upon work supported by National Science Foundation grant CMMI 2349931. Professor Michael Kinzel and Postdoctoral Fellow Jan Erik Förster are acknowledged for their support in guidance and experimentation respectively.

References

[1] Warren, P., Raju, N., Ebrahimi, H., Krsmanovic, M., Raghavan, S., Kapat, J., and Ghosh, R., "Effect of sintering temperature on microstructure and mechanical properties of molded Martian and Lunar regolith," Vol. 48, No. 23, Part B, ????, pp. 35825–35833. https://doi.org/https://doi.org/10.1016/j.ceramint.2022.07.329, URL https://www.sciencedirect.com/science/article/pii/S0272884222027560, advances in Ceramic Technologies: Materials and Manufacturing.

[2] Hampl, S. K., Austen, D. H., Van Ende, M.-A., Palečka, J., Goroshin, S., Shafirovich, E., and Bergthorson, J. M., "Conceptual design of rocket engines using regolith-derived propellants," *Acta Astronautica*, Vol. 223, 2024, pp. 594–605. https://doi.org/https://doi.org/10.1016/j.actaastro.2024.06.029, URL https://www.sciencedirect.com/science/article/pii/S0094576524003448.

[3] Torre, R., Cowley, A., and Ferro, C. G., "Low binder content bricks: a regolith-based solution for sustainable surface construction on the Moon," *Discover Applied Sciences*, Vol. 6, No. 3, 2024, p. 88.

[4] Mariani, M., Bertolini, F., Isachenkov, M., Galassi, C., Lecis, N., Grande, A., Sala, G., et al., "Binder Jetting of Lunar Regolith: 3D Printing and Densification," *75th International Astronautical Congress (IAC 2024)*, 2024, pp. 1–8.

[5] Freihofer, G., Schülzgen, A., and Raghavan, S., "Damage mapping with a degrading elastic modulus using piezospectroscopic coatings," *NDT & E International*, Vol. 75, 2015, pp. 65–71.

[6] Freihofer, G., Schülzgen, A., and Raghavan, S., "Multiscale mechanics to determine nanocomposite elastic properties with piezospectroscopy," *Acta Materialia*, Vol. 81, 2014, pp. 211–218.

[7] Stevenson, A., Jones, A., and Raghavan, S., "Stress-Sensing Nanomaterial Calibrated with Photostimulated Luminescence Emission," *Nano letters*, Vol. 11, No. 8, 2011, pp. 3274–3278. URL https://storage.cecs.ucf.edu//Groups/MMAE-Seetha/Literature/Aerostructures/Aerostructures%20Papers/Stress-Sensing%20Nanomaterial%20Calibrated%20with%20Photostimulated%20Luminescence%20Emission.pdf.

[8] Johann, M. L. S., Hoffmann, S. I. D., Greenwood, L. J., Astacio, J., Kinzel, M. P., and Raghavan, S., "Investigating the Raman Characteristics of Regolith Simulants Towards the Creation of Functional Materials," *AIAA SCITECH 2025 Forum*, 2025. https://doi.org/10.2514/6.2025-2501, URL https://arc.aiaa.org/doi/abs/10.2514/6.2025-2501.

[9] Ling, Z., Wang, A., and Jolliff, B. L., "Mineralogy and geochemistry of four lunar soils by laser-Raman study," *Icarus*, Vol. 211, No. 1, 2011, pp. 101–113. https://doi.org/https://doi.org/10.1016/j.icarus.2010.08.020, URL https://www.sciencedirect.com/science/article/pii/S001910351000326X.

[10] Zhao, H., Meng, L., Li, S., Zhu, J., Yuan, S., and Zhang, W., "Development of lunar regolith composite and structure via laser-assisted sintering," *Frontiers of Mechanical Engineering*, Vol. 17, 2022. https://doi.org/10.1007/s11465-021-0662-2.

[11] Larre, C., Morizet, Y., Guillot-Deudon, C., Baron, F., and Mangold, N., "Quantitative Raman calibration of sulfate-bearing polymineralic mixtures: a S quantification in sedimentary rocks on Mars," *Mineralogical Magazine*, Vol. 83, No. 1, 2019, p. 57–69. https://doi.org/10.1180/mgm.2018.147.

[12] Wang, A., Jolliff, B. L., and Haskin, L. A., "Raman spectroscopy as a method for mineral identification on lunar robotic exploration missions," *Journal of Geophysical Research: Planets*, Vol. 100, No. E10, 1995, pp. 21189–21199. https://doi.org/https://doi.org/10.1029/95JE02133, URL https://agupubs.onlinelibrary.wiley.com/doi/abs/10.1029/95JE02133.

[13] Freeman, J., Wang, A., Kuebler, K., Jolliff, B., and Haskin, L., "Characterization of natural feldspars by Raman spectroscopy for future planetary exploration," *The Canadian Mineralogist*, Vol. 46, 2008, pp. 1477–1500. https://doi.org/10.3749/canmin.46.6.1477.

[14] Kuebler, K. E., Jolliff, B. L., Wang, A., and Haskin, L. A., "Extracting olivine (Fo–Fa) compositions from Raman spectral peak positions," *Geochimica et Cosmochimica Acta*, Vol. 70, No. 24, 2006, pp. 6201–6222. https://doi.org/https://doi.org/10.1016/j.gca.2006.07.035, URL https://www.sciencedirect.com/science/article/pii/S0016703706019673, a Special Issue Dedicated to Larry A. Haskin.

[15] Astacio, J., Johann, M., Stein, Z., Facchini, L., Wischek, J., Bartsch, M., Kinzel, M., and Raghavan, S., "In-Space Manufacturing of Functional Sensors," *International Astronautical Congress 2024*, 2024, pp. 538–544. https://doi.org/10.52202/078356-0065.

[16] Hanhan, I., Selimov, A., Carolan, D., Taylor, A. C., and Raghavan, S., "Quantifying alumina nanoparticle dispersion in hybrid carbon fiber composites using photoluminescent spectroscopy," *Applied Spectroscopy*, Vol. 71, No. 2, 2017, pp. 258–266.

[17] Gouadec, G., and Colomban, P., "Raman Spectroscopy of nanomaterials: How spectra relate to disorder, particle size and mechanical properties," *Progress in crystal growth and characterization of materials*, Vol. 53, No. 1, 2007, pp. 1–56.

[18] Stevenson, A., Jones, A., and Raghavan, S., "Stress-Sensing Nanomaterial Calibrated with Photostimulated Luminescence Emission," *Nano Letters*, Vol. 11, No. 8, 2011, pp. 3274–3278. https://doi.org/10.1021/nl201626q, pMID: 21707042.

[19] Freihofer, G., Poliah, L., Walker, K., Medina, A., and Raghavan, S., "Optical stress probe: In-situ stress mapping with Raman and Photo-stimulated luminescence spectroscopy," *Journal of Instrumentation*, Vol. 5, 2010, p. P12003. https://doi.org/10.1088/1748-0221/5/12/P12003.